

Constraining spacetime torsion with LAGEOS

Riccardo March

Istituto per le Applicazioni del Calcolo, CNR, Via dei Taurini 19, 00185 Roma, Italy,
and INFN - Laboratori Nazionali di Frascati (LNF), via E. Fermi 40, Frascati 00044 Roma, Italy.
E-mail: r.march@iac.cnr.it

Giovanni Bellettini

Dipartimento di Matematica, Università di Roma “Tor Vergata”,
via della Ricerca Scientifica 00133 Roma, Italy,
and INFN - Laboratori Nazionali di Frascati (LNF), via E. Fermi 40, Frascati 00044 Roma, Italy.
E-mail: Giovanni.Bellettini@lnf.infn.it

Roberto Tauraso

Dipartimento di Matematica, Università di Roma “Tor Vergata”,
via della Ricerca Scientifica 00133 Roma, Italy,
and INFN - Laboratori Nazionali di Frascati (LNF), via E. Fermi 40, Frascati 00044 Roma, Italy.
E-mail: tauraso@mat.uniroma2.it

Simone Dell’Agnello

INFN - Laboratori Nazionali di Frascati (LNF), via E. Fermi 40, Frascati 00044 Roma, Italy.
E-mail: Simone.Dellagnello@lnf.infn.it

Abstract

We compute the corrections to the orbital Lense-Thirring effect (or frame-dragging) in the presence of spacetime torsion. We derive the equations of motion of a test body in the gravitational field of a rotating axisymmetric massive body, using the parametrized framework of Mao, Tegmark, Guth and Cabi. We calculate the secular variations of the longitudes of the node and of the pericenter. We also show how the LAser GEOdynamics Satellites (LAGEOS) can be used to constrain torsion parameters. We report the experimental constraints obtained using both the nodes and perigee measurements of the orbital Lense-Thirring effect. This makes LAGEOS and Gravity Probe B (GPB) complementary frame-dragging and torsion experiments, since they constrain three different combinations of torsion parameters.

Keywords: Riemann-Cartan spacetime, torsion, autoparallel trajectories, frame dragging, geodetic precession, satellite laser ranging, Gravity Probe B.

1 Introduction

In recent years a lot of effort has been devoted to measure gravitomagnetic effects due to Earth’s rotation [1], [2], [3] predicted by the theory of General Relativity (GR). In particular, the Lense-Thirring effect on the orbital motion of a test body can be measured by using the satellite laser ranging (SLR) technique, whose data are provided by the ILRS¹. By

¹International Laser Ranging Service; see <http://ilrs.gsfc.nasa.gov/>.

analyzing the laser ranging data of the orbits of the satellites LAGEOS and LAGEOS II, a measurement of the Lense-Thirring effect was obtained by Ciufolini and Pavlis [4].

SLR missions can also be useful to test modifications of GR, such as torsion theories of gravity. A class of theories allowing the presence of torsion is based on Riemann-Cartan spacetime, which is endowed with a metric $g_{\mu\nu}$ and a compatible connection. The resulting connection $\Gamma^\lambda_{\mu\nu}$ turns out to be non-symmetric, and therefore it originates a non-vanishing torsion tensor. We refer to [5], [6] for the details.

Often the source of torsion is considered to be the intrinsic spin of matter [5, 7, 8], which is negligible when averaged over a macroscopic body. Therefore spacetime torsion would be observationally negligible in the solar system. However, in [9] Mao, Tegmark, Guth and Cabi (MTGC) argue that the presence of detectable torsion in the solar system should be tested experimentally, rather than assumed by means of a specific torsion model. For this reason, in [9] a theory-independent framework based on symmetry arguments is developed, and it is determined by a set $t_1, t_2, w_1, \dots, w_5$ of seven parameters describing torsion and three further parameters $\mathcal{F}, \mathcal{G}, \mathcal{H}$ describing the metric. This parametrized framework can be used to constrain $t_1, t_2, w_1, \dots, w_5$ from solar system experiments. In particular, MTGC suggest that GPB² is an appropriate experiment for this task, and in [9] they compute precessions of gyroscopes and put consequent constraints on torsion parameters from GPB measurements.

In the present paper we compute the corrections to the orbital Lense-Thirring effect due to the presence of spacetime torsion described by $t_1, t_2, w_1, \dots, w_5$. We derive the equations of motion of a test body in the gravitational field of a rotating axisymmetric massive body. The equations of motion are obtained under the assumption of slow motion of the test body. Then we carry out the computations in the interesting cases of autoparallel and geodesic trajectories, which do not need to coincide when torsion is present.

As in the original paper of Lense and Thirring, we characterize the motion using the six orbital elements of the osculating ellipse. In terms of these orbital elements, the equations of motion then reduce to the Lagrangian planetary equations. We calculate the secular variations of the longitude Ω of the node and of the longitude $\tilde{\omega}$ of the pericenter. The computed secular variations show how the corrections to the orbital Lense-Thirring effect depend on the torsion parameters, and it turns out that the dependence is only through w_1, \dots, w_5 . The data from the LAGEOS satellites are then used to constrain the relevant linear combinations of the torsion parameters. More precisely, we constrain two different linear combinations of w_1, \dots, w_5 by using first the measurements of the nodes of LAGEOS and LAGEOS II, and then the measurements of the nodes of LAGEOS and LAGEOS II and the perigee of LAGEOS II.

Eventually, we consider the geodesic trajectories, and we find that torsion parameters cannot be constrained by satellite experiments.

While the torsion perturbations to the Lense-Thirring effect depend only on w_1, \dots, w_5 , it turns out that another relevant relativistic effect, namely the geodetic precession (or de Sitter effect), depends on the parameters t_1 and t_2 , and on a further parameter t_3 . This latter parameter is involved in a higher order parametrization of torsion, which is necessary for the description of the geodetic precession effect, while it is not necessary at the order of accuracy required in the present paper. All computations of orbital geodetic precession with torsion of a satellite are performed in the companion paper [10], to which we will sometimes refer for more details.

The paper is organized as follows. In Section 2 we briefly recall the notion of spacetime

²<http://einstein.stanford.edu/>.

with torsion. In Section 3 we recall from [9] how to parametrize the metric and torsion tensors under the assumption of axial symmetry. In Section 4 we analyze the equations of autoparallel trajectories and we derive the related system of ordinary differential equations to first order. The expression of the system clearly reveals the perturbation due to torsion with respect to the Lense-Thirring equations. In Section 5 we derive the time evolution of the orbital elements, by applying the classical perturbation theory of Celestial Mechanics, in particular the Gauss form of the Lagrange planetary equations. In Section 6 we calculate the secular variations of the orbital elements. In Section 7 we recall some results from [10] where torsion solar perturbations are computed. In Section 8 we give the observational constraints that the LAGEOS experiment can place on torsion parameters. In Section 9 we shortly analyze the geodesic trajectories.

2 Spacetime with torsion

A manifold equipped with a Lorentzian metric $g_{\mu\nu}$ and a connection $\Gamma^\lambda_{\mu\nu}$ compatible with the metric is called a Riemann-Cartan spacetime [5], [6]. Compatibility means that $\nabla_\mu g_{\nu\lambda} = 0$, where ∇ denotes the covariant derivative. We recall in particular that for any vector field v^λ

$$\nabla_\mu v^\lambda \equiv \partial_\mu v^\lambda + \Gamma^\lambda_{\mu\nu} v^\nu.$$

The connection is determined uniquely by $g_{\mu\nu}$ and by the torsion tensor

$$S_{\mu\nu}{}^\lambda \equiv \frac{1}{2} \left(\Gamma^\lambda_{\mu\nu} - \Gamma^\lambda_{\nu\mu} \right)$$

as follows:

$$\Gamma^\lambda_{\mu\nu} = \left\{ \begin{array}{c} \lambda \\ \mu\nu \end{array} \right\} - K_{\mu\nu}{}^\lambda, \quad (2.1)$$

where $\{\cdot\}$ is the Levi-Civita connection, and

$$K_{\mu\nu}{}^\lambda \equiv -S_{\mu\nu}{}^\lambda - S^\lambda_{\nu\mu} - S^\lambda_{\mu\nu} \quad (2.2)$$

is the contortion tensor. In the particular case when $\Gamma^\lambda_{\mu\nu}$ is symmetric with respect to μ, ν the torsion tensor vanishes. We will be concerned here with the case of nonsymmetric connections $\Gamma^\lambda_{\mu\nu}$. The case of vanishing torsion tensor corresponds to Riemann spacetime of GR, while the case of vanishing Riemann tensor corresponds to the Weitzenböck spacetime [11].

3 Parametrizations of metric and torsion tensors

In the present paper we use the natural gravitational units $c = 1$ and $G = 1$. In the sequel we will assume that Earth can be approximated as a uniformly rotating spherical object of mass m and angular momentum J . Following [9], we use spherical coordinates (r, θ, ϕ) for a satellite moving in the gravitational field of Earth, and we introduce the dimensionless parameters $\epsilon_m \equiv m/r$ and $\epsilon_J \equiv J/(mr)$. Since the radii of the LAGEOS orbits (about 6000 km altitude) are much larger than Earth's Schwarzschild radius, it follows that $\epsilon_m \ll 1$. Moreover, since Earth is slowly rotating, we have $\epsilon_J \ll 1$. Therefore, all computations in the present paper will be carried out perturbatively to first order in ϵ_m and ϵ_J .

Under spherical axisymmetry assumptions, the metric tensor $g_{\mu\nu}$ can be parametrized to first order as follows [9]:

$$ds^2 = - \left[1 + \mathcal{H} \frac{m}{r} \right] dt^2 + \left[1 + \mathcal{F} \frac{m}{r} \right] dr^2 + r^2 (d\theta^2 + \sin^2 \theta d\phi^2) + 2\mathcal{G} \frac{J}{r} \sin^2 \theta dt d\phi, \quad (3.1)$$

where $\mathcal{H}, \mathcal{F}, \mathcal{G}$ are three dimensionless parameters that can be immediately related to the Parametrized Post Newtonian (PPN) parameters:

$$\mathcal{H} = -2, \quad \mathcal{F} = 2\gamma, \quad \mathcal{G} = - \left(1 + \gamma + \frac{\alpha_1}{4} \right). \quad (3.2)$$

Here we follow the notation of the papers [9], [10], which will be useful in Section 7. According to [9], the torsion tensor $S_{\mu\nu}{}^\rho$ can be parametrized to first order by seven parameters $t_1, t_2, w_1, \dots, w_5$, $S_{\mu\nu}{}^\lambda = S_{\mu\nu}{}^\lambda(t_1, t_2, w_1, \dots, w_5, r, \theta, \phi)$. It turns out that parameters t_1, t_2 contribute to geodetic precession, while parameters w_1, \dots, w_5 contribute to the frame-dragging precession. The nonvanishing components of the torsion tensor are:

$$\begin{aligned} S_{tr}{}^t &= t_1 \frac{m}{2r^2}, \\ S_{r\theta}{}^\theta &= S_{r\phi}{}^\phi = t_2 \frac{m}{2r^2}, \\ S_{r\phi}{}^t &= w_1 \frac{J}{2r^2} \sin^2 \theta, \\ S_{\theta\phi}{}^t &= w_2 \frac{J}{2r} \sin \theta \cos \theta, \\ S_{t\phi}{}^r &= w_3 \frac{J}{2r^2} \sin^2 \theta, \\ S_{t\phi}{}^\theta &= w_4 \frac{J}{2r^3} \sin \theta \cos \theta, \\ S_{tr}{}^\phi &= w_5 \frac{J}{2r^4}, \\ S_{t\theta}{}^\phi &= -w_4 \frac{J \cos \theta}{2r^3 \sin \theta}. \end{aligned} \quad (3.3)$$

Therefore $\Gamma_{\mu\nu}^\lambda$ becomes an explicit function of all the torsion and metric parameters, and it has been computed in [9] and reported in the Appendix, for convenience of the reader.

4 Equations of autoparallel trajectories

Here we consider the parametrized framework of Section 3 without specifying a gravitational Lagrangian. In the absence of a Lagrangian the precise form of the equations of motion of bodies in the gravitational field is not completely specified. Therefore, following [9] we will consider the two particularly interesting cases of autoparallel and geodesic trajectories, which in general differ in the presence of torsion. Since geodesics are the same as in the PPN framework (see Section 9), new predictions related to torsion may arise only in the analysis of autoparallel trajectories. It turns out that autoparallels depend explicitly on the torsion parameters w_1, \dots, w_5 . Further motivations for investigating the autoparallel trajectories in the presence of torsion can be found in [12], [13], see also [9] and [10].

The system of equations of autoparallel trajectories reads as

$$\frac{d^2 x^\lambda}{d\tau^2} + \Gamma_{\mu\nu}^\lambda \frac{dx^\mu}{d\tau} \frac{dx^\nu}{d\tau} = 0,$$

where τ is the proper time [14]. For slow motion of the satellite we can make the substitution $d\tau \simeq dt$, so that

$$\frac{d^2 x^\alpha}{dt^2} + \Gamma^\alpha_{\mu\nu} \frac{dx^\mu}{dt} \frac{dx^\nu}{dt} = 0,$$

for $\alpha \in \{1, 2, 3\}$. We assume that the velocity of the satellite is small enough so that we can neglect the terms which are quadratic in the velocity. Then, being $x^0 = t$ we have

$$\frac{d^2 x^\alpha}{dt^2} + \Gamma^\alpha_{00} + (\Gamma^\alpha_{\beta 0} + \Gamma^\alpha_{0\beta}) \frac{dx^\beta}{dt} = 0, \quad (4.1)$$

for $\beta \in \{1, 2, 3\}$.

All the perturbations that we are considering here are so small that can be superposed linearly. Since we are only interested in the perturbations due to Earth's rotation, as in the original Lense-Thirring paper [15] we are allowed to neglect the quadratic terms in the velocities which yield an advance of the perigee of the satellite. Such an advance of the perigee in presence of torsion has been computed in [10].

We use for x^α spherical coordinates (r, θ, ϕ) . Substituting in (4.1) the expression of $\Gamma^\lambda_{\mu\nu}$ given in the Appendix one gets

$$\begin{cases} \ddot{r}r + \mathcal{C}\epsilon_m + \mathcal{D}\dot{\phi}r \sin^2 \theta \epsilon_m \epsilon_J = 0, \\ \ddot{\theta}r - \mathcal{B}\dot{\phi} \sin \theta \cos \theta \epsilon_m \epsilon_J = 0, \\ \ddot{\phi}r^2 \sin \theta + \mathcal{A}\dot{r} \sin \theta \epsilon_m \epsilon_J + \mathcal{B}\dot{\theta}r \cos \theta \epsilon_m \epsilon_J = 0, \end{cases} \quad (4.2)$$

where

$$\begin{cases} \mathcal{A} = -\mathcal{G} + w_1 - w_3, \\ \mathcal{B} = 2\mathcal{G} + w_2 - w_4, \\ \mathcal{C} = t_1 - \frac{\mathcal{H}}{2}, \\ \mathcal{D} = \mathcal{G} - w_1 - w_5. \end{cases} \quad (4.3)$$

Note that equations of motions (4.2) do not depend on the metric parameter \mathcal{F} and on the torsion parameter t_2 . System (4.2) to lowest order becomes

$$\frac{d\vec{v}}{dt} = -\mathcal{C} \frac{m}{r^2} \hat{e}_r, \quad (4.4)$$

where \hat{e}_r is the unit vector in the radial direction. Imposing the Newtonian limit it follows that (see also [9, formula (23)])

$$\mathcal{C} = 1. \quad (4.5)$$

We now transform (4.2) in rectangular coordinates $x = r \sin \theta \cos \phi$, $y = r \sin \theta \sin \phi$, $z = r \cos \theta$. We compute the second derivatives of x, y, z with respect to time in the approximation of slow motion. Neglecting all terms containing squares and products of first derivatives with respect to (r, θ, ϕ) , we get

$$\begin{cases} \ddot{x} = \ddot{r} \sin \theta \cos \phi + \ddot{\theta}r \cos \theta \cos \phi - \ddot{\phi}r \sin \theta \sin \phi, \\ \ddot{y} = \ddot{r} \sin \theta \sin \phi + \ddot{\theta}r \cos \theta \sin \phi + \ddot{\phi}r \sin \theta \cos \phi, \\ \ddot{z} = \ddot{r} \cos \theta - \ddot{\theta}r \sin \theta. \end{cases} \quad (4.6)$$

Using (4.2) and (4.6) we obtain the following system for the equations of motion:

$$\begin{cases} \ddot{x} = -\frac{\epsilon_m}{r^2}x + \frac{\epsilon_m \epsilon_J}{r^3} \left[(\mathcal{D} + \mathcal{A})xy\dot{x} + (-\mathcal{D}x^2 + \mathcal{A}y^2 + \mathcal{B}z^2)\dot{y} + (\mathcal{A} - \mathcal{B})yz\dot{z} \right], \\ \ddot{y} = -\frac{\epsilon_m}{r^2}y + \frac{\epsilon_m \epsilon_J}{r^3} \left[-(\mathcal{D} + \mathcal{A})xy\dot{y} + (-\mathcal{A}x^2 + \mathcal{D}y^2 - \mathcal{B}z^2)\dot{x} - (\mathcal{A} - \mathcal{B})xz\dot{z} \right], \\ \ddot{z} = -\frac{\epsilon_m}{r^2}z + \frac{\epsilon_m \epsilon_J}{r^3} (\mathcal{D} + \mathcal{B})z(y\dot{x} - x\dot{y}). \end{cases} \quad (4.7)$$

Note that in case of no torsion (i.e. $w_i = 0$ for any $i = 1, \dots, 5$) and when $\mathcal{G} = -2$ system (4.7) reduces to the equations of motion found by the Lense-Thirring [15, formula (15)].

5 Computation of orbital elements via perturbation theory

The system (4.7) expressing the motion along autoparallel trajectories can be written in the form

$$\begin{cases} \ddot{x} = -\frac{m}{r^3}x + F_x, \\ \ddot{y} = -\frac{m}{r^3}y + F_y, \\ \ddot{z} = -\frac{m}{r^3}z + F_z, \end{cases} \quad (5.1)$$

where (F_x, F_y, F_z) is the perturbation with respect to the Newton force,

$$\begin{cases} F_x = \frac{ma}{r^5} \left[(\mathcal{D} + \mathcal{A})xy\dot{x} + (-\mathcal{D}x^2 + \mathcal{A}y^2 + \mathcal{B}z^2)\dot{y} + (\mathcal{A} - \mathcal{B})yz\dot{z} \right], \\ F_y = \frac{ma}{r^5} \left[-(\mathcal{D} + \mathcal{A})xy\dot{y} + (-\mathcal{A}x^2 + \mathcal{D}y^2 - \mathcal{B}z^2)\dot{x} - (\mathcal{A} - \mathcal{B})xz\dot{z} \right], \\ F_z = \frac{ma}{r^5} (\mathcal{D} + \mathcal{B})z(y\dot{x} - x\dot{y}). \end{cases} \quad (5.2)$$

We use the standard coordinates transformation [16], [17] used in Celestial Mechanics

$$\begin{cases} x = r(\cos u \cos \Omega - \sin u \sin \Omega \cos i), \\ y = r(\cos u \sin \Omega + \sin u \cos \Omega \cos i), \\ z = r \sin u \sin i, \end{cases}$$

where i is the orbital inclination, Ω is the longitude of the node, and u is the argument of latitude. The vector (F_x, F_y, F_z) can be decomposed in the standard way along three mutually orthogonal axes as

$$\begin{cases} S = \frac{x}{r}F_x + \frac{y}{r}F_y + \frac{z}{r}F_z, \\ T = \frac{\partial(x/r)}{\partial u}F_x + \frac{\partial(y/r)}{\partial u}F_y + \frac{\partial(z/r)}{\partial u}F_z, \\ \sin u W = \frac{\partial(x/r)}{\partial i}F_x + \frac{\partial(y/r)}{\partial i}F_y + \frac{\partial(z/r)}{\partial i}F_z. \end{cases} \quad (5.3)$$

Here S is the component along the instantaneous radius vector, T is the component perpendicular to the instantaneous radius vector in the direction of motion, and W is the component normal to the osculating plane of the orbit (colinear with the angular momentum vector). Then, substituting (5.2) into (5.3) gives

$$\begin{cases} S = -\frac{J}{r^2} \mathcal{D} \cos i \dot{u}, \\ T = -\frac{J}{r^3} \mathcal{A} \cos i \dot{r}, \\ W = \frac{J}{r^3} \sin i (\mathcal{A} \cos u \dot{r} - \mathcal{B} \sin u r \dot{u}). \end{cases} \quad (5.4)$$

Note that in case of no torsion and when $\mathcal{G} = -2$ formulae (5.4) reduce to the components found by Lense-Thirring (see equations (16) in [15]).

Let us now recall [16], [17] that, using the method of variation of constants,

$$r = \frac{a(1 - e^2)}{1 + e \cos v},$$

where a is the semimajor axis of the satellite orbit, e is the eccentricity, v is the true anomaly, and

$$\dot{r} = \frac{r^2 e \sin v}{a(1 - e^2)} \dot{v}, \quad r^2 \dot{v} = na^2(1 - e^2)^{1/2},$$

$n = 2\pi/U$, U the period of revolution. Following the standard astronomical notation, we let ω be the argument of the perigee, and $\tilde{\omega} = \Omega + \omega$ be the longitude of the perigee.

We also recall the following planetary equations of Lagrange in the Gauss form [17, Ch. 6, Sec. 6]:

$$\begin{cases} \frac{da}{dt} = \frac{2}{n(1 - e^2)^{1/2}} \left[S e \sin v + T \frac{a(1 - e^2)}{r} \right], \\ \frac{de}{dt} = \frac{(1 - e^2)^{1/2}}{na} \left[S \sin v + T \left(e + \frac{r + a}{a} \cos v \right) \right], \\ \frac{di}{dt} = \frac{1}{na^2(1 - e^2)^{1/2}} W r \cos u, \\ \frac{d\Omega}{dt} = \frac{1}{na^2(1 - e^2)^{1/2} \sin i} W r \sin u, \\ \frac{d\tilde{\omega}}{dt} = \frac{(1 - e^2)^{1/2}}{nae} \left[-S \cos v + T \left(1 + \frac{r}{a(1 - e^2)} \right) \sin v \right] + 2 \sin^2 \frac{i}{2} \frac{d\Omega}{dt}, \\ \frac{dL_0}{dt} = -\frac{2}{na^2} S r + \frac{e^2}{1 + (1 - e^2)^{1/2}} \frac{d\tilde{\omega}}{dt} + 2(1 - e^2)^{1/2} \sin^2 \frac{i}{2} \frac{d\Omega}{dt}, \end{cases} \quad (5.5)$$

where $L_0 = -\tau n + \tilde{\omega}$ is the longitude at epoch, and τ is the time of periapsis passage.

Using the expressions of S , T and W given by (5.4) and integrating the Lagrange planetary equations we compute the variations of the orbital elements. According to perturbation

theory, we regard the orbital elements as approximately constant in the computation of such integrals. Since $u = v + \tilde{\omega} - \Omega$, we can make use of the approximation

$$\dot{u} \simeq \dot{v}. \quad (5.6)$$

Inserting (5.4)-(5.6) into (5.5) yields

$$\left\{ \begin{array}{l} \frac{da}{dt} = -\frac{2Je \cos i (1 + e \cos v)^2 \sin v}{na^2(1 - e^2)^{5/2}} (\mathcal{A}\dot{v} + \mathcal{D}\dot{u}), \\ \frac{de}{dt} = -\frac{J \cos i \sin v}{na^3(1 - e^2)^{3/2}} \left[e(e + 2 \cos v + e \cos^2 v) \mathcal{A}\dot{v} + (1 + e \cos v)^2 \mathcal{D}\dot{u} \right], \\ \frac{di}{dt} = \frac{J \sin i \cos u}{na^3(1 - e^2)^{3/2}} \left[e \sin v \cos u \mathcal{A}\dot{v} - \sin u (1 + e \cos v) \mathcal{B}\dot{u} \right], \\ \frac{d\Omega}{dt} = \frac{J \sin u}{na^3(1 - e^2)^{3/2}} \left[e \sin v \cos u \mathcal{A}\dot{v} - \sin u (1 + e \cos v) \mathcal{B}\dot{u} \right], \\ \frac{d\tilde{\omega}}{dt} = \frac{J \cos i}{na^3 e (1 - e^2)^{3/2}} \left[(1 + e \cos v)^2 \cos v \mathcal{D}\dot{u} - e \sin^2 v (2 + e \cos v) \mathcal{A}\dot{v} \right] + 2 \sin^2 \frac{i}{2} \frac{d\Omega}{dt}, \\ \frac{dL_0}{dt} = \frac{2J \cos i}{na^3(1 - e^2)} (1 + e \cos v) \mathcal{D}\dot{u} + \frac{e^2}{1 + (1 - e^2)^{1/2}} \frac{d\tilde{\omega}}{dt} + 2(1 - e^2)^{1/2} \sin^2 \frac{i}{2} \frac{d\Omega}{dt}. \end{array} \right. \quad (5.7)$$

Recalling (5.6), we now integrate (5.7) with respect to v . Therefore we find for the variations of the orbital elements:

$$\begin{aligned} \delta a &= \frac{2Je \cos i \cos v}{na^2(1 - e^2)^{5/2}} (\mathcal{A} + \mathcal{D}) \left(1 + e \cos v + \frac{1}{3} e^2 \cos^2 v \right), \\ \delta e &= \frac{J \cos i \cos v}{na^3(1 - e^2)^{3/2}} \left[(\mathcal{A} + \mathcal{D}) \left(1 + e \cos v + \frac{1}{3} e^2 \cos^2 v \right) - \mathcal{A}(1 - e^2) \right], \\ \delta i &= \frac{J \sin i}{12na^3(1 - e^2)^{3/2}} \left[4(\mathcal{A} + 2\mathcal{B})e \cos v \cos^2 u - 4(\mathcal{B} + 2\mathcal{A})e \cos v \right. \\ &\quad \left. + 2(\mathcal{B} + 2\mathcal{A})e \sin v \sin(2u) + 3\mathcal{B} \cos(2u) \right], \\ \delta \Omega &= \frac{J}{6na^3(1 - e^2)^{3/2}} \left\{ -3\mathcal{B}v + \frac{3\mathcal{B}}{2} \sin(2u) \right. \\ &\quad \left. + e \left[2(\mathcal{A} - \mathcal{B}) \sin v + (\mathcal{A} + 2\mathcal{B}) \sin(2u) \cos v - 2(2\mathcal{A} + \mathcal{B}) \sin v \cos^2 u \right] \right\}, \end{aligned}$$

$$\begin{aligned}
\delta\tilde{\omega} &= \frac{J}{na^3e(1-e^2)^{3/2}} \cos i \left\{ \sin v \left[\mathcal{D} + (\mathcal{A} + \mathcal{D})e \cos v + \frac{1}{3}(2\mathcal{D} - \mathcal{A})e^2 \right. \right. \\
&\quad \left. \left. + \frac{1}{3}(\mathcal{A} + \mathcal{D})e^2 \cos^2 v \right] + (\mathcal{D} - \mathcal{A})ev \right\} + 2 \sin^2 \frac{i}{2} \delta\Omega, \\
\delta L_0 &= \frac{2J \cos i}{na^3(1-e^2)} \mathcal{D} (v + e \sin v) + \frac{e^2}{1 + (1-e^2)^{1/2}} \delta\tilde{\omega} + 2(1-e^2)^{1/2} \sin^2 \frac{i}{2} \delta\Omega.
\end{aligned}$$

Note that, differently from the classical Lense-Thirring case, we have that δa does not vanish.

6 Torsion corrections to the Lense-Thirring effect

We observe that only periodic terms appear in δa , δe and δi . Secular terms appear in $\delta\Omega$, $\delta\tilde{\omega}$ and δL_0 . Since $v = nt +$ periodic terms in v , the secular contributions to the variations of the corresponding orbital elements are:

$$\left\{ \begin{aligned}
(\delta\Omega)_{\text{sec}} &= -\frac{J}{2a^3(1-e^2)^{3/2}} \mathcal{B}t, \\
(\delta\tilde{\omega})_{\text{sec}} &= \frac{J}{a^3(1-e^2)^{3/2}} \left[\mathcal{D} - \mathcal{A} - (\mathcal{B} + 2\mathcal{D} - 2\mathcal{A}) \sin^2 \frac{i}{2} \right] t, \\
(\delta L_0)_{\text{sec}} &= \frac{J}{a^3(1-e^2)} \left\{ 2\mathcal{D} + \frac{e^2}{1 + (1-e^2)^{1/2}} \frac{1}{(1-e^2)^{1/2}} \left[\mathcal{D} - \mathcal{A} - (\mathcal{B} + 2\mathcal{D} - 2\mathcal{A}) \sin^2 \frac{i}{2} \right] \right. \\
&\quad \left. - (\mathcal{B} + 4\mathcal{D}) \sin^2 \frac{i}{2} \right\} t.
\end{aligned} \right. \tag{6.1}$$

In the absence of torsion and when $\mathcal{G} = -2$, it turns out that $(\delta\tilde{\omega})_{\text{sec}} = (\delta L_0)_{\text{sec}}$, as found by Lense-Thirring.

Using (4.3) we rewrite (6.1). For the nodal rate we obtain

$$(\delta\Omega)_{\text{sec}} = -\frac{\mathcal{G}J}{a^3(1-e^2)^{3/2}} (1 + \mu_1) t, \tag{6.2}$$

and for the longitudinal rate of the perigee

$$(\delta\tilde{\omega})_{\text{sec}} = \frac{2\mathcal{G}J}{a^3(1-e^2)^{3/2}} \left[1 + \mu_2 - 3(1 + \mu_3) \sin^2 \frac{i}{2} \right] t. \tag{6.3}$$

Since $\tilde{\omega} = \Omega + \omega$, for the rate of the argument of the perigee we find

$$(\delta\omega)_{\text{sec}} = \frac{\mathcal{G}J}{a^3(1-e^2)^{3/2}} \left[3 + \mu_1 + 2\mu_2 - 6(1 + \mu_3) \sin^2 \frac{i}{2} \right] t. \tag{6.4}$$

The parameters

$$\begin{aligned}\mu_1 &\equiv \frac{w_2 - w_4}{2\mathcal{G}}, \\ \mu_2 &\equiv \frac{2w_1 - w_3 + w_5}{-2\mathcal{G}}, \\ \mu_3 &\equiv \frac{4w_1 - w_2 - 2w_3 + w_4 + 2w_5}{-6\mathcal{G}},\end{aligned}$$

measure deviations from GR. Indeed, when there is no torsion we have $w_i = 0$ for $i = 1, \dots, 5$. When, in addition, $\mathcal{G} = -2$ the metric is the weak field approximation of a Kerr-like metric, and $\mu_1 = \mu_2 = \mu_3 = 0$ and we get the classical Lense-Thirring formulae [15]. We also give the expression for the rate of the longitude at epoch, namely

$$\begin{aligned}(\delta L_0)_{\text{sec}} = & -\frac{2\mathcal{G}J}{a^3(1-e^2)} \left\{ -\frac{e^2}{1+(1-e^2)^{1/2}} \frac{1}{(1-e^2)^{1/2}} (1+\mu_2) - (1+\mu_4) \right. \\ & \left. + \left[(1+\mu_1) + \frac{3e^2}{1+(1-e^2)^{1/2}} \frac{1}{(1-e^2)^{1/2}} (1+\mu_3) + 2(1+\mu_4) \right] \sin^2 \frac{i}{2} \right\} t,\end{aligned}\tag{6.5}$$

where

$$\mu_4 \equiv \frac{w_1 + w_5}{-\mathcal{G}}.$$

Note that μ_1, \dots, μ_4 do not depend on $t_1, t_2, \mathcal{F}, \mathcal{H}$. The fact that the secular variations depend only on the parameters w_i is in agreement with the results of [9] dealing with gyroscopes. Indeed, the geodetic precession of gyroscopes depends only on $t_1, t_2, \mathcal{F}, \mathcal{H}$, while the frame-dragging precession depends on the remaining parameters w_1, \dots, w_5 and \mathcal{G} .

7 Torsion corrections to the geodetic precession

The secular perturbations of the orbital elements computed in the previous sections are not the only torsion induced perturbations that are expected. Indeed, a further contribution due to solar perturbation is present, namely the geodetic precession in presence of torsion. In the paper [10] the geodetic precession of orbital elements of the satellite in the gravitational field of the Earth and the Sun (both supposed to be nonrotating) is computed, in a Sun-centered reference system. It is shown that, to the required order of accuracy, the corresponding metric takes the form

$$ds^2 = -h(r)dt^2 + f(r)dr^2 + r^2[d\theta^2 + \sin^2\theta d\phi^2],\tag{7.1}$$

where

$$h(r) = 1 + \mathcal{H}\frac{M}{r} + \mathcal{I}\frac{M^2}{r^2}, \quad f(r) = 1 + \mathcal{F}\frac{M}{r},\tag{7.2}$$

and the nonvanishing components of the torsion tensor take the form

$$\begin{aligned}S_{tr}{}^t &= t_1 \frac{M}{2r^2} + t_3 \frac{M^2}{r^3}, \\ S_{r\theta}{}^\theta &= S_{r\phi}{}^\phi = t_2 \frac{M}{2r^2} + t_4 \frac{M^2}{r^3},\end{aligned}\tag{7.3}$$

where M is the mass of the Sun, \mathcal{I} is a dimensionless parameter, and t_3 and t_4 are arbitrary dimensionless constants. In the case of a PPN metric we have

$$\mathcal{I} = 2(\beta - \gamma), \quad (7.4)$$

where β is the usual PPN parameter.

The secular contributions to the precessions of the node and of the perigee due to torsion found in [10] are the following:

$$(\delta\Omega^{\text{Sun}})_{\text{sec}} = \frac{1}{4} \frac{M\nu_0}{\rho} \left(C_1 - C_2 \frac{\nu_0}{n} \cos i \right) t, \quad (7.5)$$

$$(\delta\tilde{\omega}^{\text{Sun}})_{\text{sec}} = \frac{1}{4} \frac{M\nu_0}{\rho} \left\{ C_1 + C_2 \frac{\nu_0}{n} [4 - \cos i - 5 \sin^2 i \sin^2(\tilde{\omega} - \Omega)] \right\} t,$$

where

$$C_1 \equiv 1 - \frac{\mathcal{H}}{2} + 2\mathcal{F} + 3t_2, \quad C_2 \equiv 1 + \frac{\mathcal{H}}{2} + \frac{\mathcal{H}^2}{2} - \mathcal{F} - \mathcal{I} + t_2 + 2t_3, \quad (7.6)$$

ν_0 is the revolution angular velocity of the Earth around the Sun, and ρ is the distance of the Earth from the Sun.

Differently from the Lense-Thirring effect, the precessions (7.5) depend on the torsion parameters t_2 and t_3 , and are independent of t_4 ; the parameter t_1 is identified using the Newtonian limit (4.5).

We recall that t_3 and t_4 enter the parametrization of torsion at the higher order of accuracy required in the computation of precessions (7.5), see [10] for the details.

The perturbations (7.5) have to be superimposed to the ones computed in Section 6.

The first term on the right hand sides of the two formulas in (7.5) can be interpreted as the geodetic precession effect, when torsion is present [10]: accordingly we set

$$(\delta\Omega^{\text{geo}})_{\text{sec}} = (\delta\tilde{\omega}^{\text{geo}})_{\text{sec}} = \frac{C_1}{4} \frac{M\nu_0}{\rho} t. \quad (7.7)$$

In the PPN formalism we have

$$C_1 = 2 + 4\gamma + 3t_2, \quad C_2 = t_2 + 2(1 - \beta + t_3).$$

Using lunar laser ranging (LLR) data and Mercury radar ranging data respectively, the following upper bounds are given in [10, Section 13]:

$$|t_2| < 0.0128, \quad |1 - \beta + t_3| < 0.0286. \quad (7.8)$$

Since for LAGEOS satellites $\frac{\nu_0}{n} \sim 4.2 \times 10^{-4}$, we have

$$(\delta\Omega^{\text{Sun}})_{\text{sec}} \simeq (\delta\Omega^{\text{geo}})_{\text{sec}}, \quad (\delta\tilde{\omega}^{\text{Sun}})_{\text{sec}} \simeq (\delta\tilde{\omega}^{\text{geo}})_{\text{sec}}.$$

Taking into account the expression of C_1 , we have

$$(\delta\Omega^{\text{geo}})_{\text{sec}} = (\delta\tilde{\omega}^{\text{geo}})_{\text{sec}} = \frac{M\nu_0}{2\rho} \left(1 + 2\gamma + \frac{3}{2}t_2 \right) t. \quad (7.9)$$

This formula yields the rate of geodetic precession around an axis which is normal to the ecliptic plane. The projection of this precession rate on the axis of rotation of Earth is obtained by multiplying $(\delta\Omega^{\text{geo}})_{\text{sec}}$ by $\cos \epsilon$, where $\epsilon = 23.5$ degrees is the angle between the Earth's equatorial plane and the ecliptic plane [18]: this gives the values of the geodetic precession in a Earth-centered reference system.

8 Constraining torsion parameters with LAGEOS

In this section we describe how the LAGEOS data can be used to extract a limit on the torsion parameters. We will assume in the following that all metric parameters take the same form as in the PPN formalism, according to (3.2) and (7.4).

8.1 Constraints from nodes measurement

Here we discuss how frame dragging torsion parameters can be constrained by the measurement of a suitable linear combination of the nodal rates of the two LAGEOS satellites.

Equation (6.2) can be rewritten as

$$(\delta\Omega)_{\text{sec}} = \frac{2J}{a^3(1-e^2)^{3/2}} \left(-\frac{\mathcal{G}}{2} - \frac{w_2 - w_4}{4} \right) t = (\delta\Omega)_{\text{sec}}^{\text{GR}} b_{\Omega}, \quad (8.1)$$

where we have defined, similarly to [9] and [10], a multiplicative torsion ‘‘bias’’ relative to the GR prediction as

$$b_{\Omega} = \frac{(\delta\Omega)_{\text{sec}}}{(\delta\Omega)_{\text{sec}}^{\text{GR}}} = -\frac{\mathcal{G}}{2} - \frac{w_2 - w_4}{4} = \frac{1}{2} \left(1 + \gamma + \frac{\alpha_1}{4} \right) - \frac{w_2 - w_4}{4}, \quad (8.2)$$

$(\delta\Omega)_{\text{sec}}^{\text{GR}} = \frac{2J}{a^3(1-e^2)^{3/2}}$ being the Lense-Thirring precession in GR. We recall that the values of such precessions are 31mas/yr and 31.5mas/yr for LAGEOS and LAGEOS II, respectively, where mas/yr denotes milli-arcseconds per year.

Let us now consider the contribution of the geodetic precession to the nodal rate. We write the secular contribution to the nodal rate, in a Earth-centered reference system, in the form

$$(\delta\Omega^{\text{geo}})_{\text{sec}} \cos \epsilon = (\delta\Omega^{\text{geo}})_{\text{sec}}^{\text{GR}} \cos \epsilon b_{\Omega}^{\text{geo}}, \quad (8.3)$$

where b_{Ω}^{geo} depends on t_2 . Precisely, taking into account that $(\delta\Omega^{\text{geo}})_{\text{sec}}^{\text{GR}} = \frac{3M\nu_0}{2\rho} t$ and using (7.9), we have

$$b_{\Omega}^{\text{geo}} = \frac{1}{3}(1 + 2\gamma) + \frac{t_2}{2}. \quad (8.4)$$

Moreover, the following numerical constraints are set on PPN parameters γ and α_1 by Cassini tracking [19] and LLR data [3], respectively:

$$\gamma - 1 = (2.1 \pm 2.3) \times 10^{-5}, \quad |\alpha_1| < 10^{-4}. \quad (8.5)$$

From (8.5) it follows that the term $\frac{1}{3}(1 + 2\gamma)$ differs from 1 by a few part in 10^{-5} . Therefore, using (7.8), (8.4) and (8.5) we get

$$|b_{\Omega}^{\text{geo}} - 1| \simeq \left| \frac{t_2}{2} \right| < 0.0064. \quad (8.6)$$

The measurement of the Lense-Thirring effect in [4], [20] is based on the following linear combination of the total nodal rates of the two LAGEOS satellites:

$$\delta\Omega_{\text{I}}^{\text{tot}} + \kappa\delta\Omega_{\text{II}}^{\text{tot}}, \quad (8.7)$$

where the subscripts I and II denote LAGEOS and LAGEOS II, respectively. Here the total nodal rate $\delta\Omega^{\text{tot}}$ of a LAGEOS satellite denotes the nodal rate due to all kinds of

perturbations, both gravitational and nongravitational. The coefficient $\kappa = 0.545$ is chosen to make the linear combination (8.7) independent of any contribution of the Earth's quadrupole moment J_2 , which describes the Earth's oblateness.

In [4] the residual (observed minus calculated) nodal rates $\Delta(\delta\Omega_I)$, $\Delta(\delta\Omega_{II})$ of the LAGEOS satellites are obtained analyzing nearly eleven years of laser ranging data. The residuals are then combined according to the linear combination $\Delta(\delta\Omega_I) + \kappa\Delta(\delta\Omega_{II})$, analogue to (8.7). The Lense-Thirring effect is set equal to zero in the calculated nodal rates. The linear combination of the residuals, after removal of the main periodic signals, is fitted with a secular trend which corresponds to 99% of the theoretical Lense-Thirring prediction of GR (see [4], [20] for the details):

$$(\delta\Omega_I)_{\text{sec}}^{\text{GR}} + \kappa(\delta\Omega_{II})_{\text{sec}}^{\text{GR}} = 48.2 \text{ mas/yr.}$$

The total uncertainty of the measurement is approximately $\pm 10\%$ of the value predicted by GR [4], [20].

Using the upper bound (8.6), the uncertainty in modeling geodetic precession in the presence of torsion is

$$|b_{\Omega}^{\text{geo}} - 1| \left[(\delta\Omega_I^{\text{geo}})_{\text{sec}}^{\text{GR}} + \kappa(\delta\Omega_{II}^{\text{geo}})_{\text{sec}}^{\text{GR}} \right] \cos \epsilon \leq 0.0064 \frac{27.2}{48.2} \left[(\delta\Omega_I)_{\text{sec}}^{\text{GR}} + \kappa(\delta\Omega_{II})_{\text{sec}}^{\text{GR}} \right], \quad (8.8)$$

where $\left[(\delta\Omega_I^{\text{geo}})_{\text{sec}}^{\text{GR}} + \kappa(\delta\Omega_{II}^{\text{geo}})_{\text{sec}}^{\text{GR}} \right] \cos \epsilon = 27.2 \text{ mas/yr}$ is the contribution from geodetic precession predicted by GR for LAGEOS satellites. Compared to the $\pm 10\%$ uncertainty in the measurement of the Lense-Thirring effect, the uncertainty in modeling geodetic precession can be neglected (as in [4], [20]) even in the presence of spacetime torsion. This is a consequence of the torsion limits set with the Moon and Mercury in [10].

Then we can apply the results of [4], [20] to our computations with torsion, and we obtain

$$\left| (\delta\Omega_I)_{\text{sec}} + \kappa(\delta\Omega_{II})_{\text{sec}} - 0.99 \left[(\delta\Omega_I)_{\text{sec}}^{\text{GR}} + \kappa(\delta\Omega_{II})_{\text{sec}}^{\text{GR}} \right] \right| < 0.10 \left[(\delta\Omega_I)_{\text{sec}}^{\text{GR}} + \kappa(\delta\Omega_{II})_{\text{sec}}^{\text{GR}} \right],$$

where $(\delta\Omega_I)_{\text{sec}}$ and $(\delta\Omega_{II})_{\text{sec}}$ are given by (8.1). Since the torsion bias b_{Ω} does not depend on the orbital elements of the satellite, we have

$$\frac{(\delta\Omega_I)_{\text{sec}} + \kappa(\delta\Omega_{II})_{\text{sec}}}{(\delta\Omega_I)_{\text{sec}}^{\text{GR}} + \kappa(\delta\Omega_{II})_{\text{sec}}^{\text{GR}}} = b_{\Omega}.$$

Hence, using (8.2), we can constrain a linear combination of the frame-dragging torsion parameters w_2 , w_4 , setting the limit

$$|b_{\Omega} - 0.99| = \left| \frac{1}{2} \left(\gamma - 1 + \frac{\alpha_1}{4} \right) - \frac{w_2 - w_4}{4} + 0.01 \right| < 0.10,$$

which is shown graphically in fig. 8.1, together with the other constraints on γ and α_1 [3]. Taking into account the numerical constraints (8.5) the limit on torsion parameters from LAGEOS becomes

$$\left| -\frac{w_2 - w_4}{2} + 0.02 \right| < 0.20$$

which implies

$$-0.36 < w_2 - w_4 < 0.44. \quad (8.9)$$

One of the goals of the LAGEOS, LAGEOS II, LARES³ three-satellite experiment, together with improved Earth's gravity field models of GRACE (Gravity Recovery And Climate

³LASer RELativity Satellite, a geodynamics mission of the Italian Space Agency (ASI) to be launched.

Experiment) is to improve the experimental accuracy on the orbital Lense-Thirring effect to “a few percent” [20].

We observe that, using (8.8) the uncertainty in modelling geodetic precession in the presence of torsion amounts to about 0.4% of the Lense-Thirring effect, which is still a small contribution to a total root-square-sum error of a few percent. Note that an improved determination of the geodetic precession is expected by GPB which, unlike LAGEOS, is designed to separate the frame-dragging and geodetic precessions by measuring two different, orthogonal precessions of its gyroscopes.

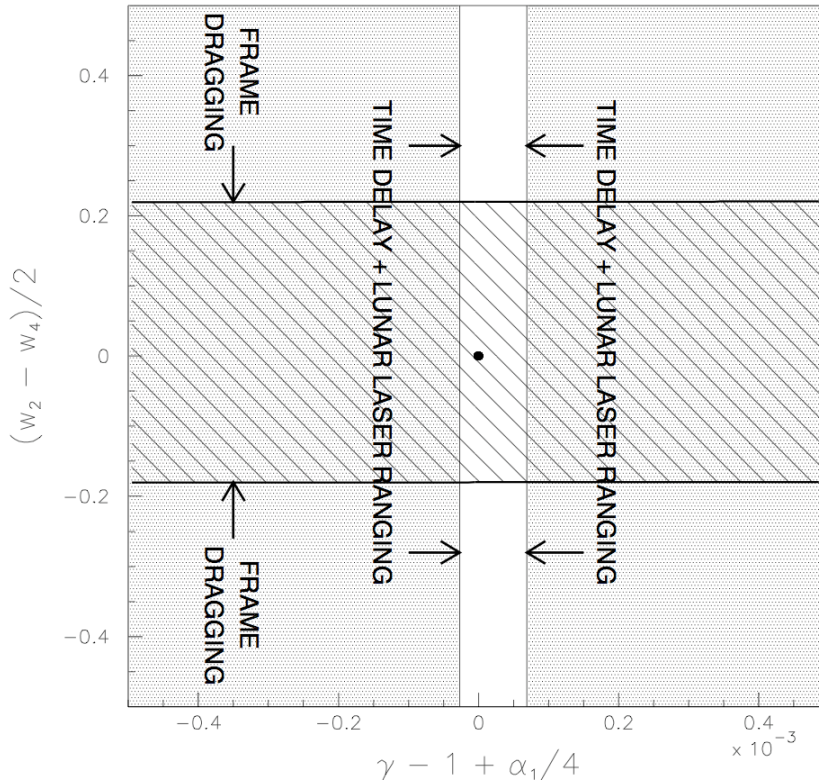


Figure 1: constraints on PPN parameters (γ, α_1) and on frame-dragging torsion parameters (w_2, w_4) from solar system tests. The grey area is the region excluded by lunar laser ranging and Cassini tracking. The LAGEOS nodes measurement of the Lense-Thirring effect [4], [20] excludes values of $(w_2 - w_4)/2$ outside the hatched region. General Relativity corresponds to $\gamma = 1$, $\alpha_1 = 0$ and all torsion parameters = 0 (black dot).

In the case of GPB, the torsion bias for the precession of a gyroscope is [9]

$$-\frac{\mathcal{G}}{2} - \frac{w_1 + w_2 - w_3 - 2w_4 + w_5}{2}.$$

This formula (the analogue of the right hand side of equation (8.2)) involves a linear combination of all frame-dragging torsion parameters. Such a linear combination can be constrained from GPB data. Since LAGEOS and GPB are sensitive to different linear combinations, together they can put more stringent torsion limits.

After taking into account the contribution of the geodetic precession, the combined constraints from gyroscope and orbital Lense-Thirring experiments are effective probes to search

for the experimental signatures of spacetime torsion. In this sense, LAGEOS and GPB are to be considered complementary frame-dragging and, at the same time, torsion experiments, with the notable difference that GPB can measure also the geodetic precession.

8.2 Constraints from nodes and perigee measurement

In this section we discuss how frame dragging torsion parameters can be constrained by the measurement of a linear combination of the nodal rates of LAGEOS and LAGEOS II and the perigee rate of LAGEOS II.

Similarly to the previous section, we define a multiplicative torsion “bias” relative to the GR prediction also for the rate of the argument of the perigee (6.4):

$$b_\omega = \frac{(\delta\omega)_{\text{sec}}}{(\delta\omega)_{\text{sec}}^{\text{GR}}} = -\frac{\mathcal{G}}{6 \cos i} \left[3 + \mu_1 + 2\mu_2 - 6(1 + \mu_3) \sin^2 \frac{i}{2} \right],$$

$(\delta\omega)_{\text{sec}}^{\text{GR}} = -\frac{6J \cos i}{a^3(1-e^2)^{3/2}}$ being the Lense-Thirring precession in GR: we recall that the value of this precession is -57mas/yr for LAGEOS II. In the following, the torsion bias b_ω is referred to LAGEOS II.

Using the values of μ_1 , μ_2 and μ_3 given in Section 6 we find

$$b_\omega = -\frac{\mathcal{G}}{2} + \frac{4w_1 - w_2 - 2w_3 + w_4 + 2w_5}{12}. \quad (8.10)$$

The measurement of the Lense-Thirring effect in [21] is based on the following linear combination of the residuals of the nodes of LAGEOS and LAGEOS II and of the perigee of LAGEOS II:

$$\Delta(\delta\Omega_{\text{I}}) + c_1\Delta(\delta\Omega_{\text{II}}) + c_2\Delta(\delta\omega_{\text{II}}), \quad (8.11)$$

where the coefficients $c_1 = 0.295$ and $c_2 = -0.35$ are chosen to make the linear combination (8.11) independent of the first two even zonal harmonic coefficients J_2 and J_4 , and of their uncertainties.

In [21] the residuals are obtained analyzing four years of laser ranging data, and then combined according to the linear combination (8.11). The Lense-Thirring effect is set equal to zero in the calculated rates of the nodes and of the perigee. The linear combination of the residuals, after removal of the main periodic signals and of small observed inclination residuals, is fitted with a secular trend which corresponds to 1.1 times the theoretical Lense-Thirring prediction of GR (see [21] for the details):

$$(\delta\Omega_{\text{I}})_{\text{sec}}^{\text{GR}} + c_1(\delta\Omega_{\text{II}})_{\text{sec}}^{\text{GR}} + c_2(\delta\omega_{\text{II}})_{\text{sec}}^{\text{GR}} = 60.2 \text{ mas/yr}.$$

The total uncertainty of the measurement found in [21] is $\pm 20\%$ of the value predicted by GR. The contribution to such an uncertainty due to nongravitational perturbations, mainly thermal perturbative effects, on the perigee of LAGEOS II, amounts to 13% of the value predicted by GR. In [22] such an estimate is confirmed, however the author, when considering more pessimistic assumptions on some thermal effects, estimates that the contribution of nongravitational perturbations to the total uncertainty does not exceed the 28% of the GR value. Here we will follow this more conservative estimate. Inserting this value in the estimate of the total uncertainty computed in [21] yields a total root-square-sum error of 32% of the GR value.

For reasons similar to the ones discussed in the previous section, we are allowed to neglect the uncertainty in modeling the geodetic precession in the presence of torsion. Then we can apply the results of [21] to our computations with torsion, and we obtain

$$\begin{aligned} & \left| (\delta\Omega_{\text{I}})_{\text{sec}} + c_1(\delta\Omega_{\text{II}})_{\text{sec}} + c_2(\delta\omega_{\text{II}})_{\text{sec}} - 1.1 [(\delta\Omega_{\text{I}})_{\text{sec}}^{\text{GR}} + c_1(\delta\Omega_{\text{II}})_{\text{sec}}^{\text{GR}} + c_2(\delta\omega_{\text{II}})_{\text{sec}}^{\text{GR}}] \right| \\ & < 0.32 [(\delta\Omega_{\text{I}})_{\text{sec}}^{\text{GR}} + c_1(\delta\Omega_{\text{II}})_{\text{sec}}^{\text{GR}} + c_2(\delta\omega_{\text{II}})_{\text{sec}}^{\text{GR}}]. \end{aligned}$$

A direct computation gives

$$|(1 - K)b_\Omega + Kb_\omega - 1.1| < 0.32, \quad (8.12)$$

where

$$K = \frac{c_2(\delta\omega_{\text{II}})_{\text{sec}}^{\text{GR}}}{(\delta\Omega_{\text{I}})_{\text{sec}}^{\text{GR}} + c_1(\delta\Omega_{\text{II}})_{\text{sec}}^{\text{GR}} + c_2(\delta\omega_{\text{II}})_{\text{sec}}^{\text{GR}}} = 0.33.$$

Inserting in (8.12) the expressions of b_Ω and b_ω given in (8.2), (8.10) and taking into account that $\mathcal{G} \simeq -2$ by formula (8.5), we obtain

$$-0.22 < -\frac{w_2 - w_4}{4} + K \left(\frac{2w_1 + w_2 - w_3 - w_4 + w_5}{6} \right) < 0.42.$$

Using the value of K we finally deduce

$$-0.22 < 0.11w_1 - 0.20w_2 - 0.06w_3 + 0.20w_4 + 0.06w_5 < 0.42, \quad (8.13)$$

which is shown graphically in fig. 8.2, together with the other constraints on γ and α_1 [3]. The constraint (8.13) on the linear combination of the frame-dragging parameters is rather weak, due to the uncertainty on the nongravitational perturbations. Notice that the coefficients in front of w_3 and w_5 are of an order of magnitude smaller than the coefficients of the other parameters, so that the constraint on w_3 and w_5 is even looser.

Thermal thrusts (TTs) are the main source of non-gravitational perturbations [22]. One of the main drivers of LAGEOS TTs is the thermal relaxation time τ_{CCR} of its fused silica cube corner retroreflectors [23], which has been characterized in laboratory-simulated space conditions at the INFN-LNF Satellite/lunar laser ranging Characterization Facility (SCF) [24], [25], [26]. The measurements of LAGEOS τ_{CCR} in a variety of thermal conditions provide the basis for possibly reducing the uncertainty on the thermal perturbative effects. As a consequence, the constraint (8.13) could be improved.

We recall that in [9] an upper bound on the combination $|w_1 + w_2 - w_3 - 2w_4 + w_5|$ is given. This constrains the torsion parameters to lie between two parallel hyperplanes in a five-dimensional space. If we couple this bound with our two estimates (8.9) and (8.13), it follows that w_1, \dots, w_5 are constrained to lie in a five-dimensional set, which is unbounded only along two directions. Hence, coupling GPB with LLR measurements reduces the degrees of freedom on the frame-dragging parameters in a significative manner.

We conclude this section by observing that the recently approved JUNO mission to Jupiter [27] will make it possible, in principle, to attempt a measurement of the Lense-Thirring effect through the JUNO's node, which would be displaced by about 570 metres over the mission duration of one year [28]. Hence, such a mission yields an opportunity for a possible improvement of the constraints on torsion parameters.

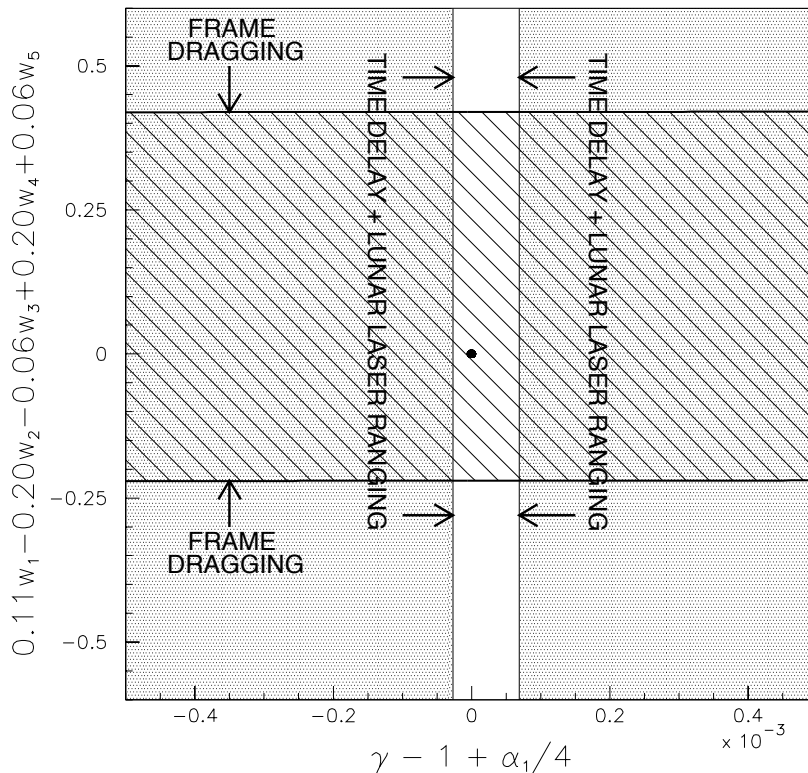


Figure 2: constraints on PPN parameters (γ, α_1) and on frame-dragging torsion parameters $(w_1, w_2, w_3, w_4, w_5)$ from solar system tests. The grey area is the region excluded by lunar laser ranging and Cassini tracking. The LAGEOS nodes and perigee measurement of the Lense-Thirring effect [21], [22] excludes values of $0.11w_1 - 0.20w_2 - 0.06w_3 + 0.20w_4 + 0.06w_5$ outside the hatched region. General Relativity corresponds to $\gamma = 1$, $\alpha_1 = 0$ and all torsion parameters = 0 (black dot).

9 Equations of geodesics

In this section we consider the particular case of geodesic trajectories. The system of equations of geodesic trajectories reads as

$$\frac{d^2 x^\lambda}{d\tau^2} + \left\{ \begin{array}{c} \lambda \\ \mu\nu \end{array} \right\} \frac{dx^\mu}{d\tau} \frac{dx^\nu}{d\tau} = 0.$$

The resulting equations of motion is given by (4.2) with

$$A = -\mathcal{G}, \quad B = 2\mathcal{G}, \quad C = -\frac{\mathcal{H}}{2}, \quad D = \mathcal{G}.$$

Imposing the Newtonian limit to the equations of motion to lowest order (4.4), we have $\mathcal{H} = -2$. The nodal rate and the longitudinal rate of the perigee become

$$(\delta\Omega)_{\text{sec}} = -\frac{\mathcal{G}J}{a^3(1-e^2)^{3/2}} t, \quad (\delta\tilde{\omega})_{\text{sec}} = (\delta L_0)_{\text{sec}} = \frac{2\mathcal{G}J}{a^3(1-e^2)^{3/2}} \left(1 - 3\sin^2 \frac{i}{2}\right) t. \quad (9.1)$$

From (3.2) it follows that $\frac{d\Omega}{dt}$ and $\frac{d\tilde{\omega}}{dt}$ depend only on the PPN parameters of the metric. Note that when $\mathcal{G} = -2$ the expressions in (9.1) reduce (to lowest order) to the classical corresponding Lense-Thirring quantities. Therefore the measurements of satellite experiments cannot be used to constrain the torsion parameters.

10 Conclusions

We have applied the framework recently developed in [9] for GR with torsion, to the computation of the slow orbital motion of a satellite in the field generated by the Earth. Starting from the autoparallel trajectories, we computed the corrections to the classical orbital Lense-Thirring effect in the presence of torsion. By using perturbation theory, we have found the explicit dependence of the secular variations of the longitudes of the node and of the perigee on the frame-dragging torsion parameters. The LAGEOS nodes measurements [4], [20] and the LAGEOS nodes and perigee measurements [21], [22] of the Lense-Thirring effect can be used to place constraints on torsion parameters, which are different and complementary to those set by GPB.

11 Appendix

The expression of the nonvanishing components of the connection approximated to first order in $\epsilon_m = m/r$, $\epsilon_J = J/(mr)$ and $\epsilon_m\epsilon_J = J/r^2$ is the following [9]:

$$\begin{aligned} \Gamma^t_{tr} &= \frac{1}{2r} (2t_1 - \mathcal{H}) \epsilon_m \\ \Gamma^t_{rt} &= -\frac{\mathcal{H}}{2r} \epsilon_m \\ \Gamma^t_{r\phi} &= \frac{1}{2} (3\mathcal{G} + (w_1 - w_3 - w_5)) \sin^2 \theta \epsilon_m \epsilon_J \\ \Gamma^t_{\phi r} &= \frac{1}{2} (3\mathcal{G} - (w_1 + w_3 + w_5)) \sin^2 \theta \epsilon_m \epsilon_J \\ \Gamma^t_{\theta\phi} &= \frac{1}{2} w_2 r \sin \theta \cos \theta \epsilon_m \epsilon_J \\ \Gamma^r_{tt} &= \frac{1}{2r} (2t_1 - \mathcal{H}) \epsilon_m \\ \Gamma^r_{rr} &= -\frac{\mathcal{F}}{2r} \epsilon_m \\ \Gamma^r_{\theta\theta} &= -r + (t_2 + \mathcal{F}) r \epsilon_m \\ \Gamma^r_{\phi\phi} &= -r \sin^2 \theta + \frac{1}{r} (\mathcal{F} + t_2) \sin^2 \theta \epsilon_m \\ \Gamma^r_{t\phi} &= \frac{1}{2} (\mathcal{G} - (w_1 - w_3 + w_5)) \sin^2 \theta \epsilon_m \epsilon_J \\ \Gamma^r_{\phi t} &= \frac{1}{2} (\mathcal{G} - (w_1 + w_3 + w_5)) \sin^2 \theta \epsilon_m \epsilon_J \end{aligned}$$

$$\begin{aligned}
\Gamma_{t\phi}^{\theta} &= -\frac{1}{2r}(2\mathcal{G} + (w_2 - 2w_4)) \sin\theta \cos\theta \epsilon_m \epsilon_J \\
\Gamma_{\phi t}^{\theta} &= -\frac{1}{2r}(2\mathcal{G} + w_2) \sin\theta \cos\theta \epsilon_m \epsilon_J \\
\Gamma_{r\theta}^{\theta} &= \Gamma_{r\phi}^{\phi} = \frac{1}{r} \\
\Gamma_{\theta r}^{\theta} &= \Gamma_{\phi r}^{\phi} = \frac{1}{r} - \frac{1}{r} t_2 \epsilon_m \\
\Gamma_{\phi\phi}^{\theta} &= -\sin\theta \cos\theta \\
\Gamma_{tr}^{\phi} &= -\frac{1}{2r^2}(\mathcal{G} - (w_1 - w_3 + w_5)) \epsilon_m \epsilon_J \\
\Gamma_{rt}^{\phi} &= -\frac{1}{2r^2}(\mathcal{G} - (w_1 - w_3 - w_5)) \epsilon_m \epsilon_J \\
\Gamma_{t\theta}^{\phi} &= \frac{1}{2r}(2\mathcal{G} + (w_2 - 2w_4)) \frac{\cos\theta}{\sin\theta} \epsilon_m \epsilon_J \\
\Gamma_{\theta t}^{\phi} &= \frac{1}{2r}(2\mathcal{G} + w_2) \frac{\cos\theta}{\sin\theta} \epsilon_m \epsilon_J \\
\Gamma_{\theta\phi}^{\phi} &= \Gamma_{\phi\theta}^{\phi} = \frac{\cos\theta}{\sin\theta}
\end{aligned}$$

12 Acknowledgments

We thank the University of Roma ‘‘Tor Vergata’’, CNR and INFN for supporting this work. We thank I. Ciufolini for suggesting this analysis after the publication of the paper by MTGC [9], and B. Bertotti and A. Riotto for useful advices.

References

- [1] I. Ciufolini, J.A. Wheeler, *Gravitation and Inertia*, Princeton Univ. Press, Princeton (1995).
- [2] C.M. Will, *Theory and Experiment in Gravitational Physics*, Cambridge Univ. Press (1993).
- [3] C.M. Will, *Living Rev. Relativity* **9**, 3 (2006) (www.livingreviews.org/lrr-2006-3).
- [4] I. Ciufolini, E.C. Pavlis, *Nature* **431**, 958 (2004).
- [5] F.W. Hehl, P. von der Heyde, G.D. Kerlick, J.M. Nester, *Rev. Mod. Phys.* **48**, 393 (1976).
- [6] R.T. Hammond, *Rep. Prog. Phys.* **65**, 599 (2002).
- [7] W.R. Stoeger, P.B. Yasskin, *Gen. Rel. Gravit.* **11**, 427 (1979).
- [8] P.B. Yasskin, W.R. Stoeger, *Phys. Rev. D* **21**, 2081 (1980).
- [9] Y. Mao, M. Tegmark, A.H. Guth, S. Cabi, *Phys. Rev. D* **76**, 1550 (2007).
- [10] R. March, G. Bellettini, R. Tauraso, S. Dell’Agnello, submitted paper.
- [11] K. Hayashi, T. Shirafuji, *Phys. Rev. D* **19**, 3524 (1979).

- [12] H. Kleinert, A. Pelster, *Gen. Rel. Grav.* **31**, 1439 (1999).
- [13] T. Dereli, R.W. Tucker, *Mod. Phys. Lett. A* **17**, 421 (2002).
- [14] V.N. Ponomarev, *Bull. Acad. Polon. Sci.* **XIX**, 6 (1971).
- [15] J. Lense, H. Thirring, *Phys. Z.* **19**, 156 (1918), translated in: B. Mashhoon, F. Hehl, D.S. Theiss, *Gen. Rel. Grav.* **16**, No. 8 (1984).
- [16] D. Brouwer, G.M. Clemence, *Methods of Celestial Mechanics*, Academic Press (1961).
- [17] F.T. Geyling, H.R. Westerman, *Introduction to Orbital Mechanics*, Addison Wesley (1971).
- [18] C. Huang, J.C. Ries, B.D. Tapley, M.M. Watkins, *Celestial Mech. Dyn. Astron.* **48**, 167 (1990).
- [19] B. Bertotti, L. Iess, P. Tortora, *Nature* **425**, 374 (2003).
- [20] I. Ciufolini et al., *Sp. Sci. Rev.*, **148** 71 (2009)
- [21] I. Ciufolini, E. Pavlis, F. Chieppa, E. Fernandes-Vieira, J. Pérez-Mercader, *Science* **279**, 2100 (1998).
- [22] D.M. Lucchesi, *Plan. Space Sci.* **50**, 1067 (2002).
- [23] A. Bosco, C. Cantone, S. Dell’Agnello, G. O. Delle Monache et al., *Int. J. Mod. Phys. D* **16-12a**, 2271 (2007).
- [24] S. Dell’Agnello et al., in “Proceedings of the 16th International Workshop on Laser Ranging” (2008), October 13-17, Poznan, Poland, 121.
- [25] S. Dell’Agnello et al., *Adv. Space Res.*, *Galileo Special Issue*, DOI 10.1016/j.asr.2010.10.022 (2010).
- [26] S. Dell’Agnello et al., *Exp. Astron.*, *MAGIA Special Issue*, DOI 10.1007/s10686-010-9195-0 (2010).
- [27] S. Matousek, *Acta Astronautica* **61**, 932 (2007).
- [28] L. Iorio, *New Astronomy* **15**, 554 (2010).